Investigational New Drugs (2020) 38:574–583
https://doi.org/10.1007/s10637-019-00806-3

PRECLINICAL STUDIES

The influence of the coadministration of the p-glycoprotein modulator elacridar on the pharmacokinetics of lapatinib and its distribution in the brain and cerebrospinal fluid

Agnieszka Karbownik[1] · Katarzyna Sobańska[1] · Włodzimierz Płotek[2] · Tomasz Grabowski[3] · Agnieszka Klupczynska[4] · Szymon Plewa[4] · Edmund Grześkowiak[1] · Edyta Szałek[1]

Received: 29 January 2019 / Accepted: 28 May 2019 / Published online: 8 June 2019

Summary

Background Lapatinib is a small-molecule tyrosine kinase inhibitor of human epidermal receptor 2 (HER2) and EGFR that has currently been approved for the treatment of HER2-positive advanced and metastatic breast cancer (BC). The ATP-binding cassette (ABC) family of transporters includes P-glycoprotein (P-gp; ABCB1) and breast cancer resistance protein (BCRP; ABCG2), which substantially restrict the penetration of drugs, including chemotherapeutics, through the blood-brain barrier and blood-cerebrospinal fluid barrier. The aim of this study was to investigate the effects of elacridar, an ABCB1 and ABCG2 inhibitor, on the brain and cerebrospinal fluid uptake of lapatinib. *Methods* Rats were divided into two groups: one group received 5 mg/kg elacridar and 100 mg/kg lapatinib (an experimental group), and the other group received 100 mg/kg lapatinib (a control group). Lapatinib concentrations in the blood plasma (BP), cerebrospinal fluid (CSF) and brain tissue (BT) were measured by liquid chromatography coupled with tandem mass spectrometry. *Results* Elacridar significantly increased lapatinib penetration into the CSF and BT (C_{max} increase of 136.4% and 54.7% and $AUC_{0-\infty}$ increase of 53.7% and 86.5%, respectively). The C_{max} of lapatinib in BP was similar in both experimental groups (3057.5 vs. 3257.5 ng/mL, respectively). *Conclusion* This study showed that elacridar influenced the pharmacokinetics of lapatinib. The inhibition of ABCB1 and ABCG2 transporters by elacridar substantially enhanced the penetration of lapatinib into the CSF and BT. The blocking of protein transporters could become indispensable in the treatment of patients with breast cancer and brain metastases.

Keywords Lapatinib · Elacridar · Blood-brain barrier · Blood-cerebrospinal fluid barrier

Introduction

Breast cancer (BC) is the most common malignant cancer diagnosed in women in Europe and the US. Distant metastases are a major threat in the course of the disease [1]. BC is the second most common tumor (following lung cancer) with brain metastases (BM). Approximately 6–16% of patients with BC have metastases within the central nervous system (CNS) [2, 3]. The treatment of BC patients with BM remains a difficult therapeutic problem. The appearance of metastases in the CNS always results in poor prognosis [4–7]. The average survival time of untreated patients is only one month, whereas radiotherapy applied to the CNS extends the survival time to 3–6 months. Even patients with a single CNS lesion who undergo surgery and radiotherapy live only slightly longer, i.e., 10–16 months. The percent of clinically apparent BM is significantly higher (24–48%) in patients with HER2 receptor

Electronic supplementary material The online version of this article (https://doi.org/10.1007/s10637-019-00806-3) contains supplementary material, which is available to authorized users.

✉ Agnieszka Karbownik
agnieszkakarbownik@o2.pl

[1] Department of Clinical Pharmacy and Biopharmacy, Poznań University of Medical Sciences, ul. Św. Marii Magdaleny 14, 61-861 Poznań, Poland

[2] Department of Anaesthesiology and Intensive Therapy Teaching, Poznań University of Medical Sciences, ul. Św. Marii Magdaleny 14, 61-861 Poznań, Poland

[3] Polpharma Biologics, ul. Trzy Lipy 3, 80-172 Gdańsk, Poland

[4] Department of Inorganic and Analytical Chemistry, Poznań University of Medical Sciences, ul. Grunwaldzka 6, 60-780 Poznań, Poland

overexpression [8]. The survival time of these patients is longer than the survival time of patients that are HER2(−). Trastuzumab is a first-line drug used to treat patients with HER2-positive BM. However, due to the high molecular weight of trastuzumab (145,531 Da), its ability to cross the blood-brain barrier (BBB) is limited. Therefore, small-molecule tyrosine kinase inhibitors (TKIs), such as lapatinib, have been the subject of numerous clinical trials to evaluate their effectiveness in women with HER2(+) BM [9, 10].

The results of molecular studies led to the expectation that lapatinib could be successfully applied to BC patients with BM because of its theoretical ability to cross the BBB, as a result of its very low molecular weight (581 Da). Lapatinib was proven to be the first TKI that blocks HER2 receptors and significantly reduces the number of BM [11–13]. Unfortunately, only approximately 2.6–6.0% of patients with BM respond to lapatinib therapy [14]. This minimal therapeutic effect may be caused by the low bioavailability of the drug in the target tissue. This may partly result from the activity of P-glycoprotein (P-gp; ABCB1) and breast cancer resistance protein (BCRP; ABCG2), which are present in the BBB. As these proteins significantly restrict lapatinib penetration into the brain, it is necessary to examine a therapeutic strategy that will overcome this blockade and thus increase the distribution of lapatinib in BM. Therefore, the aim of this study was to assess the influence of elacridar, a third-generation ABCB1 inhibitor, on brain and CSF exposure to lapatinib in rats.

Materials and methods

Reagents

Lapatinib (CAS number 231277–92-9), formic acid, methanol, acetonitrile, ammonium formate, and dimethyl sulfoxide (DMSO) were purchased from Sigma-Aldrich (Poznań, Poland). Erlotinib (CAS number 183321–74-6) and elacridar (CAS number 143664–11-3) were purchased from LGC Standards (Łomianki, Poland). Water used in the mobile phase was deionized, distilled and filtered through a Millipore system (Direct Q3, Merck Millipore, Burlington) before use. Lapatinib (Tyverb®, batch number Y68Y) and 0.9% NaCl (batch number 15BO4G61) were purchased from Novartis Polska Sp. z o.o., (Warsaw, Poland) and Baxter Polska Sp. z o.o. (Warsaw, Poland), respectively.

Animals

This study was conducted on rats, which are a promising model to predict P-gp-based drug-drug interactions at the human BBB [15]. The animals were allowed to acclimate for one week before the beginning of the experiments. Adult male Wistar-strain rats (weight 470–525 g) were used in the study. The animals were maintained under standard breeding conditions with a 12/12 h light-dark cycle (lights on at 6.00 a.m., lights off at 6.00 p.m.) at constant room temperature (23 ± 2 °C), relative humidity (55 ± 10%) and ad libitum access to food and water. The experimental protocol for this study was reviewed and approved by the Local Ethics Committee. To obtain consistent data, the study was based on the required minimum number of animals and observation time. The rats were divided into two groups: one receiving elacridar and lapatinib (I_{E+L}) and the other receiving lapatinib (II_L). Three rats were used at each time point ($n = 3$). In total, the research was conducted on 66 animals ($n = 33$ in the experimental group and n = 33 in the control group). Twenty-two animals were excluded from the research ($n = 11$ from the experimental group and n = 11 from the control group) because their CSF was stained with blood.

Drug administration and sample collection

Elacridar was freshly dissolved in a vehicle at an initial concentration of 20 mg/mL. This solution was administered intraperitoneally at a dose of 5 mg/kg 30 min prior to lapatinib administration [16]. Lapatinib (100 mg/kg b.w. [17]) was dissolved in 1 mL of 10% DMSO and administered with a gastric probe directly into the rats' stomach. A volume of 80 μL of blood was collected from each rat by cutting off a piece of its tail. The blood samples were collected into heparinized test tubes at the following time points: before treatment (time 0), 5 min, 30, min, and 1, 2, 3, 4, 6, 8, 12, and 24 h after administration of the drugs, and they were immediately centrifuged at 2880 *g* for 10 min at 4 °C. The anaesthetized rats (anaesthetized by intramuscular administration of 50 mg/kg ketamine and 10 mg/kg xylazine) were prepared for cisterna magna puncture. The hair over the puncture was removed and the skin was disinfected with alcohol. The animals were placed in a recumbent position with an elevated rear part of the body. The animals' heads were slightly flexed and immobilized with the operator's left hand. The space between the occiput rostrally and the atlas (C1) of the spinal column caudally was gently palpated with the left thumb. A 0.7 × 20 G needle with polyethylene tubing (Terumo Poland, Warsaw, Poland) was gently inserted at an approximate angle of 80–90° through the skin with the operator's right hand into the midsagittal region. The moment that dura mater perforation was perceptible, a small amount of CSF was found in the needle tubing. To sample additional CSF, a 1 mL insulin syringe (Becton Dickinson, Warsaw, Poland) was used to collect 80–120 μL of CSF by very gentle aspiration. Only clear CSF was collected for further analysis. At each time point, one animal had to be rejected from the analysis because the collected CSF was stained with blood. The animals' brains were immediately dissected, washed in 0.9% NaCl and divided along the longitudinal axis. One of the brain hemispheres

was again rinsed three times with 5 mL of 0.9% NaCl, weighed and homogenized with 0.9% NaCl (4 mL per 1 g of BT) in an Ultra-Turrax homogenizer (Witko, Łódź, Poland). The homogenate was then centrifuged at 4500 *g* for 10 min. All samples of the rat BP, CSF, and BT homogenate supernatant were stored at −80 °C until analysis.

Lapatinib measurements

The concentrations of lapatinib in rat BP, CSF and BT homogenates were measured using a validated HPLC method coupled with tandem mass spectrometry (HPLC-MS/MS). The chromatographic analysis was conducted using a 1260 Infinity system (Agilent Technologies, Santa Clara, USA) equipped with a Kinetex® C18 column (50 × 4.6 mm, 2.6 μm, Phenomenex, Torrance, USA), which was maintained at 35 °C. The mobile phase consisted of 0.1% formic acid (*v*/*v*) in water with 5 mM ammonium formate (solvent A) and acetonitrile with 10% phase A (*v*/*v*, solvent B). The analyte and internal standard (IS, erlotinib) were eluted using a gradient run of 10 min as follows: 95% A at 0–2 min; 95%–5% A at 2–4 min; 5% A at 4–5 min; 5%–95% A at 5–6 min; 95% A at 6–10 min. The flow rate and injection volume were set at 0.7 mL/min and 10 μL, respectively. The needle was washed for 30 s in a mixture of acetonitrile, methanol, isopropanol, water, and formic acid (50:20:15:15:0.25, *v*/*v*/*v*/*v*/*v*). A 4000 QTRAP triple quadrupole mass spectrometer (Sciex, Framingham, USA) with an electrospray ionization (ESI) source was operated in multiple reaction monitoring mode. The ESI source parameters were as follows: ion spray voltage - 4000.0 V; nitrogen curtain gas - 45.0 psi; temperature - 500 °C; ion source gas 1–50.0 psi; ion source gas 2–40.0 psi. Positive ionization mode and a dwell time of 160.0 ms were used for all transitions monitored. The following precursor-ion-to-product-ion transitions were measured: *m/z* 581.1 → 365.1 (collision energy, CE 55 eV), *m/z* 581.1 → 350.1 for lapatinib (CE 55 eV) and *m/z* 394.1 → 278.1 for IS (CE 46 eV).

Rat BP (20 μL) was mixed with 50 μL of the IS solution (100 ng/mL) and 930 μL of methanol and then vortexed for 30 s (total dilution factor of 50). After centrifugation at 14,300 *g* (2 min), the supernatant was transferred into an HPLC vial and injected onto the HPLC column.

CSF (20 μL) was added to 10 μL of the IS solution (100 ng/mL) and 170 μL of methanol, vortexed for 30 s, and then centrifuged at 14,300 *g* for 2 min. Next, the supernatant was analyzed by means of the HPLC-MS/MS system. A total dilution factor of 10 was measured.

Rat BT homogenates were diluted with ultrapure water (1:1, *m*/*m*). Then, an aliquot (40 μL) was mixed with 50 μL of the IS solution (100 ng/mL) and 910 μL of methanol, which yielded a total dilution factor of 50. The mixture was vortexed rigorously for 30 s and centrifuged at 14,300 *g* for 2 min. The resulting supernatant was injected onto the HPLC-MS/MS system.

Data acquisition and processing were controlled with Analyst 1.5.2 software (Sciex, Framingham, USA). The calibration curves were prepared within a range of 0.25–150.0 ng/mL with a correlation coefficient $r > 0.99$. The lower limit of quantification (LLOQ) was determined at 0.25 ng/mL with acceptable precision and accuracy and $S/N > 10$. The accuracy, determined as %bias, was ≤13% across three quality control (QC) levels and < 20% for the LLOQ. The intra- and inter-run precision of the assay (coefficient of variation) was within 15% for the QC samples and below 20% for the LLOQ. Stability experiments with low and high QC samples showed that lapatinib was stable for three freeze-thaw cycles at −80 °C (deviation <5%) and for three months of storage at −80 °C (deviation <15%). Moreover, the postpreparative stability of lapatinib in both BP samples and standard solutions showed no significant change in the concentration (<15%) after 24 h and 48 h of storage in the autosampler at 4 °C.

Pharmacokinetic analysis

Noncompartmental analysis and the sparse sampling technique in the Phoenix® WinNonlin® 8.0 software (Certara L.P.) were used to calculate the pharmacokinetic parameters on the basis of lapatinib concentration in the rat BP, CSF, and BT. The maximum concentration (C_{max}) and the time to reach the maximum plasma concentration (t_{max}) were calculated directly from the concentration-time data. The elimination rate constant (k_{el}) was estimated from the slope of the terminal linear segment of the log mean concentration-time plot using the automatic best-fitting option in WinNonlin 8.0. The elimination half-life ($t_{0.5}$) was calculated from the $\ln 2/k_{el}$. The area under the concentration-time curve from zero to the time of the last concentration measured ($AUC_{0\text{-}t}$) was calculated by the linear trapezoidal rule. The residual area under the curve (AUC_{res}) was estimated by extrapolation from the last concentration measured (C_{last}) to infinity using the C_{last}/k_{el} ratio. The area under the curve from zero to infinity ($AUC_{0\text{-}\infty}$) was computed as the sum of $AUC_{0\text{-}t}$ and AUC_{res}. The total concentrations in BT were corrected for the analytes present in residual brain blood using the method described by Fridén et al. [18]: $C_{b,corr} = [C_b - (f_{u,p} \cdot V_w \cdot C_p + (1\text{-}f_{u,p}) \cdot V_{protein} \cdot C_p)]/[1 - V_w]$, where $C_{b,corr}$ denotes the total concentration of the compound in an individual rat brain corrected for the residual blood; C_b is the total concentration measured in an individual rat brain; C_p is the mean of the total plasma concentration of the analyte observed in the rats of a given sex and age at the same time as in the brain; $f_{u,p}$ is the unbound fraction of the compound in plasma; and V_w and $V_{protein}$ are the apparent brain vascular spaces of plasma water (10.3 mL/g) and plasma proteins (8.0 mL/g), respectively. The tissue-to-plasma partition coefficient (K_p) was calculated as $AUC_{0\text{-}\infty\text{-}tissue}/AUC_{0\text{-}\infty\text{-}plasma}$.

The tissue uptake efficiency and selectivity were assessed with K_p, and the drug targeting index (DTI) was calculated as $K_{p\ I(E+L)}/K_{pII(L)}$ [19]. Additionally, the hysteresis-like plots correlating the plasma concentration with the tissue concentration and the corresponding calculated r^2 values were analyzed.

Results

Concentration-time profiles of lapatinib in BP, CSF, and BT

Figures 1, 2 and 3 show time-dependent changes in the mean concentration of lapatinib in the BP, CSF and BT, respectively. After 24 h, the concentration of lapatinib in each matrix sample in the II_L group was undetectable. The levels of lapatinib were below the LLOQ in 20 CSF samples.

Plasma pharmacokinetic parameters of lapatinib

The pharmacokinetic profile of lapatinib in BP differed between the two groups. The lapatinib plasma $AUC_{0\text{-}t}$ and $AUC_{0\text{-}\infty}$ where 78.7% and 155.6% higher in the I_{E+L} when compared to the II_L group (Table 1). The C_{max} of lapatinib was greater by 6.3% and occurred earlier in the I_{E+L} group (2.50 vs. 4.00 h). Moreover, the $t_{0.5}$ of lapatinib was 5.2-fold prolonged when the drug was coadministered with elacridar.

Tissue uptake

The effect of elacridar on lapatinib tissue distribution was evaluated in the CSF and BT. The C_{max} of lapatinib in the CSF was 2.4-fold increased in the I_{E+L} group when compared to the control group (I_L) (Table 1). Similarly, 1.55-fold increase of lapatinib C_{max} in the I_{E+L} group was observed in BT. The $AUC_{0\text{-}t}$ and $AUC_{0\text{-}\infty}$ of lapatinib in the CSF were elevated by 61.2% and by 53.7% in the I_{E+L} group. Likewise, the exposure to lapatinib in BT was higher in the I_{E+L} group than in the II_L group ($AUC_{0\text{-}t}$ and $AUC_{0\text{-}\infty}$ increased by 92.6% and 86.5%, respectively). The elimination of lapatinib was additionally extended in the presence of elacridar, as the lapatinib $t_{0.5}$ in the CSF and BT was 2.6 times and 2.5 times longer, respectively.

Tissue uptake efficiency

The uptake efficiency of lapatinib in the CSF and BT was higher in the II_L group than in the I_{E+L} group. The lapatinib K_p in the I_{L+E} group was decreased by 42.9% in the CSF and by 25% in the BT when compared to the control group (Table 1). This effect could also be seen in the hysteresis-like plots (Fig. 5), where r^2 increased slightly in the CSF from 0.0183 in the control group (I_L) to 0.1665 in the I_{E+L} group. However, the r^2 value decreased in the BT (0.2109 in the I_{E+L} group vs. 0.7751 in the I_L group) (Fig. 4). The BT data above do not allow us to draw conclusions about drug penetration at different doses and concentrations of lapatinib (Fig. 5).

Discussion

Few anticancer drugs, including cytotoxic and molecularly targeted agents (e.g., TKIs), are sufficiently effective for the treatment of brain tumors. Although the response rate of targeted drugs currently appears to be higher than that observed with conventional chemotherapy in certain subtypes of molecular metastases to BT, it is still insufficient to ensure desirable treatment results. The limited therapeutic potential of available agents against tumors located in BT mainly results from their scarce distribution throughout the BBB. The BBB is characterized by the presence of membrane transporters (e.g., P-gp and

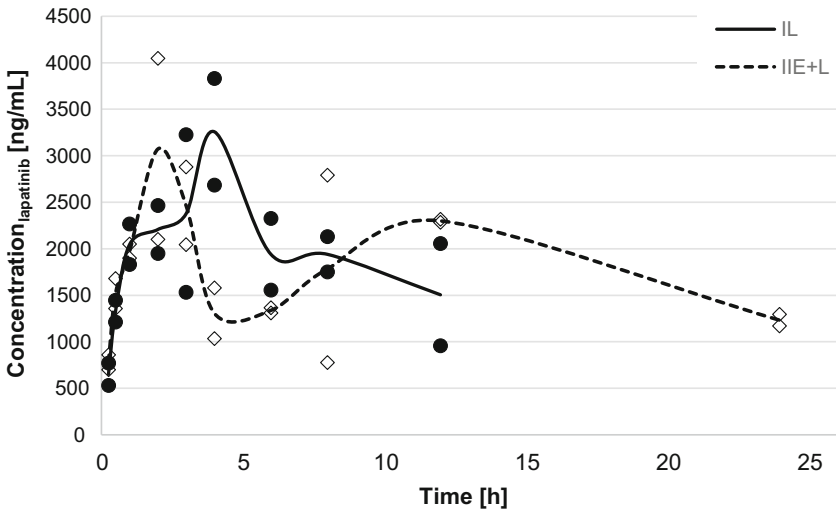

Fig. 1 The blood plasma (BP) concentration-time profiles of lapatinib after a single oral dose (100 mg/kg) in the II_L ($n = 2$) and I_{E+L} groups (n = 2)

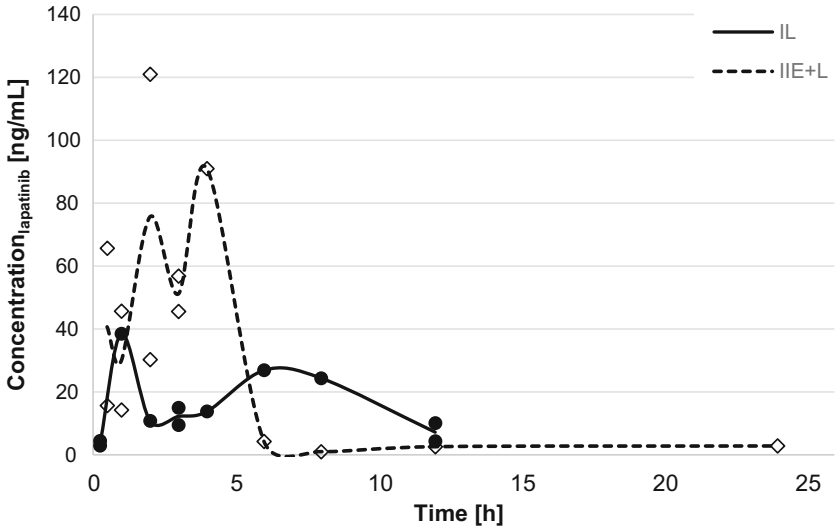

Fig. 2 The cerebrospinal fluid (CSF) concentration-time profiles of lapatinib after a single oral dose (100 mg/kg) in the II_L and I_{E+L} groups

BCRP), which are responsible for the efflux of many drugs, including TKIs [20]. However, research has proven that TKIs, such as lapatinib, erlotinib, gefitinib, afatinib, crizotinib, and alectinib, in combination with cytotoxic drugs or alone, are potent in reducing the development of CNS tumors [21–26]. Lapatinib is a substrate for P-gp and BCRP, which are abundantly expressed in the intestine, liver, kidney and BBB [27]. This drug was also identified as an inhibitor of P-gp, BCRP, and OATP (organic anion transporting polypeptide) [28]. Therefore, the knowledge of interactions between lapatinib and these transporters enables an assessment of the possibility of drug penetration into crucial targeted tissues. The inhibition of P-gp-mediated drug efflux has already been recognized as an attractive target for therapeutic intervention to treat multidrug resistant cancers. Elacridar is a potent inhibitor of the proteins ABCB1 and ABCG2 [21, 29]. The inhibited transporters affect the absorption of TKIs in the intestine, their hepatic and renal excretion and penetration through the BBB. The expression levels and activity of P-gp and BCRP are strongly associated with the limited distribution of most TKIs to the BT [22]. Research has shown that brain accumulation of axitinib, cediranib and crizotinib depends mainly on ABCB1 activity, whereas the brain disposition of sorafenib is predominantly influenced by the ABCG2 protein [23].

Plasma pharmacokinetic parameters of lapatinib

In our study, the coadministration of elacridar substantially change the exposition of lapatinib (Fig. 1). The C_{max} of lapatinib was 6.3% higher in the I_{E+L} group than in the II_L group. This may be explained by the fact that systemic exposure to lapatinib is not dependent on gastrointestinal P-gp and BCRP activity. Polli et al. proved that plasma AUC, C_{max} and t_{max} values of lapatinib in rats pretreated with elacridar were similar to the values observed in vehicle-treated animals [28]. However, in our study the AUC_{0-t} and $AUC_{0-\infty}$ of lapatinib

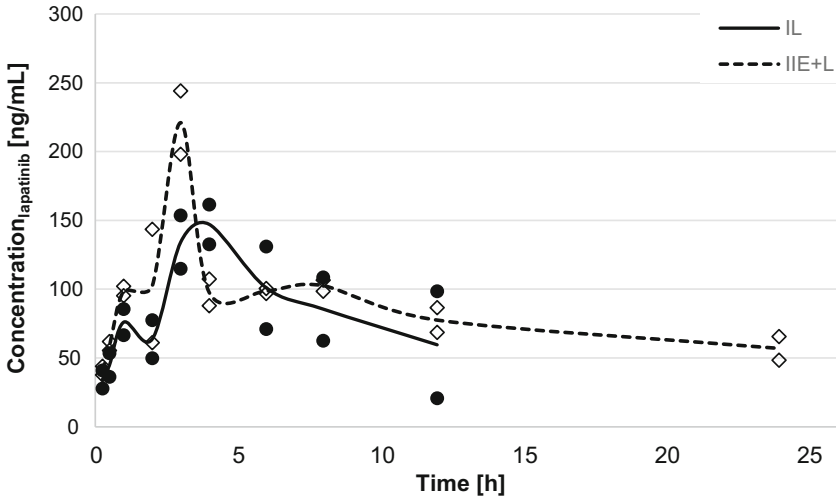

Fig. 3 The brain tissue (BT) concentration-time profiles of lapatinib after a single oral dose (100 mg/kg) in the II_L (n = 2) and I_{E+L} groups (n = 2)

Table 1 The noncompartmental plasma pharmacokinetic parameters of lapatinib after oral administration of 100 mg/kg (II_L) or coadministration with 5 mg/kg of elacridar (I_{E+L})

Pharmacokinetic parameters	I_{L+E}	II_L
Blood plasma (BP)[a]		
C_{max} (ng/mL)	3462.50 ± 823.78	3257.50 ± 809.64
t_{max} (h)	2.50 ± 0.71	4.00 ± 0.00
k_{el} (h^{-1})	0.02 ± 0.01	0.13 ± 0.03
$t_{0.5}$ (h)	28.77 ± 6.00	5.58 ± 1.28
AUC_{0-t} (ng × h/mL)	43,556.06 ± 3905.44	24,377.19 ± 125.07
$AUC_{0-\infty}$ (ng × h/mL)	95,087.03 ± 10,426.84	37,197.82 ± 9150.67
$AUMC_{0-t}$ (ng × h^2/mL)	480,290.03 ± 21,589.07	138,877.66 ± 11,299.79
$AUMC_{0-\infty}$ (ng × h^2/mL)	3,917,566.05 ± 1,363,043.99	404,148.02 ± 215,793.89
MRT_{0-t} (h)	11.05 ± 0.50	5.70 ± 0.43
Cerebrospinal fluid (CSF)		
C_{max} (ng/mL)	91.00	38.50
t_{max} (h)	4.0	1.0
k_{el} (h^{-1})	0.09	0.23
$t_{0.5}$ (h)	7.69	3.00
AUC_{0-t} (ng × h/mL)	355.83	220.76
$AUC_{0-\infty}$ (ng × h/mL)	387.33	252.03
$AUMC_{0-t}$ (ng × h^2/mL)	1620.02	1257.21
$AUMC_{0-\infty}$ (ng × h^2/mL)	2725.51	1767.90
MRT_{0-t} (h)	4.55	5.70
K_p	0.004	0.007
Brain tissue (BT)[a]		
C_{max} (ng/mL)	197.67 ± 39.01	127.76 ± 16.38
k_{el} (h^{-1})	0.05 ± 0.02	0.25 ± 0.24
$t_{0.5}$ (h)	13.01 ± 3.99	5.29 ± 5.11
t_{max} (h)	3.00 ± 0.00	4.50 ± 2.12
AUC_{0-t} (ng × h/mL)	1610.22 ± 130.95	836.10 ± 21.20
$AUC_{0-\infty}$ (ng × h/mL)	2520.56 ± 610.81	1351.27 ± 712.37
MRT_{0-t} (h)	9.92 ± 1.04	5.73 ± 0.06
$AUMC_{0-t}$ (ng × h^2/mL)	16,040.19 ± 2981.02	4792.63 ± 173.92
$AUMC_{0-t}$ (ng × h^2/mL)	57,148.33 ± 29,162.29	17,455.77 ± 17,542.73
K_p	0.027	0.036

C_{max} – maximum concentration; t_{max} – time to C_{max}; k_{el} – elimination rate constant; AUC_{0-t} – area under the plasma concentration-time curve from zero to the time of the last measurable concentration; $AUC_{0-\infty}$ – area under the plasma concentration-time curve from zero to infinity; $t_{0.5}$ – elimination half-life; MRT_{0-t} – mean residence time; $AUMC_{0-t}$ – area under the first moment curve from zero to the time of the last measurable concentration; $AUMC_{0-\infty}$ – area under the first moment curve from zero to infinity; K_p – tissue-to-plasma partition coefficient;
[a] – arithmetic means ± standard deviations

were 78.7% and 155.6% greater than in the II_L group (Table 1). Elacridar is highly bound to plasma proteins (in rats: 99.0 ± 0.6% [30], 98.1 ± 1.7 [16]), therefore it could have displaced lapatinib from its plasma protein binding, increasing its free fraction in blood. This could also have resulted in prolonged elimination of lapatinib in the presence of elacridar. The higher exposure to lapatinib might be at least in part a result of the fact that pharmacokinetic calculations were made in I_{E+L} group up to 24 h. In the II_L group last measurable point was 12 h, therefore AUC values in this group were underestimated when compared to the I_{E+L} group.

Tissue uptake and efficiency in cerebrospinal fluid

Elacridar increased the lapatinib C_{max} and $AUC_{0-\infty}$ in the CSF 2.4-fold and 1.5-fold, respectively (Table 1). The lapatinib $C_{max,CSF}/C_{max,BP}$ ratio proved to be higher in the I_{E+L} group than in the II_L group (0.026 vs. 0.012) and the $C_{max,CSF,IE+L}/C_{max,CSF,IIL}$ ratio amounted to 2.4. Gorgi [26] presented a case report of 2 patients treated with lapatinib in combination with capecitabine due to BC with BM (HER2+). Five hours after the oral administration of 1250 mg of lapatinib, the drug concentrations in the BP were 1515 and 3472 ng/mL in the one

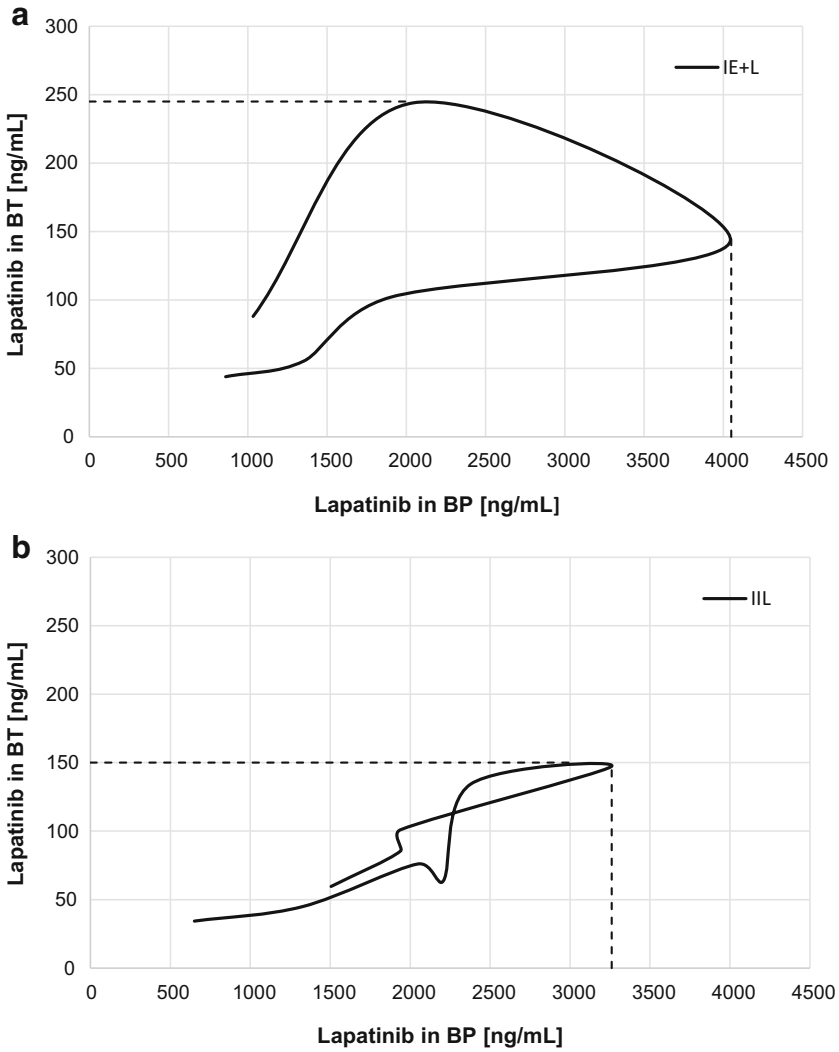

Fig. 4 The comparative hysteresis-like plots of the lapatinib concentration in brain tissue (BT) versus blood plasma (BP) for the I_{E+L} group, $r^2 = 0.2109$ (**a**) and for the II_L group, $r^2 = 0.7751$ (**b**)

and another patient, whereas the drug concentration in CSF amounted to 1.3 and 4.5 ng/mL, respectively. The lapatinib $C_{CSF,5h}/C_{BP,5h}$ ratios for these two patients were 0.00086 and 0.0013. The authors concluded that the low concentration of lapatinib in the CSF and low ratios may have resulted from the poor solubility of lapatinib in water and low concentrations of proteins in the CSF. In addition, the experiment showed that the concentration of lapatinib in the CSF is not be a reliable indicator of CNS drug penetration.

Tissue uptake and efficiency in brain tissue

Elacridar significantly increased the lapatinib C_{max} and $AUC_{0-\infty}$ in BT 1.5 times and 1.9 times, respectively (Table 1). After the administration of elacridar with another TKI, sunitinib, the penetration of the TKI to the brain was enhanced [19]. The brain-to-plasma ratio of sunitinib in the WT mice after concomitant administration of elacridar was comparable to the brain-to-plasma ratio observed in the knockout mice *(mdr1a/b$^{(-/-)}$;bcrp1$^{(-/-)}$)*. These data allowed us to conclude that sunitinib penetration to the brain may be increased by the administration of a dual P-gp/BCRP inhibitor. These data can be used to plan clinical trials on patients with brain tumors, e.g., with *glioblastoma multiforme*. Lagas et al. [24] observed that *abcb1a/lb;abcg2$^{(-/-)}$* mice had the most pronounced increase in dasatinib concentration in the brain, which was 13.2 times greater after oral administration and 22.7 times greater after intraperitoneal administration. Moreover, the coadministration of elacridar and dasatinib to WT mice resulted in a similar accumulation of dasatinib in the brain as for *abcb1a/1b,abcg2$^{(-/-)}$* mice. The brain-to-plasma ratio in the WT mice increased 4.4 times with elacridar, but the presence of this P-gp/BCRP inhibitor did not produce similar increase in the P-gp and BCRP knockout mice. Tang et al. [25] showed that *abcb1a/1b$^{(-/-)}$* and *abcb1a/1b;abcg2$^{(-/-)}$* mice experienced approximately 2 times higher BP exposure to low doses of crizotinib (5 mg/kg b.w.) than WT mice. Additionally, the brain accumulation of crizotinib after 24 h was approximately 40 times greater in the WT mice, whereas when the dose was increased ten-fold, the brain accumulation

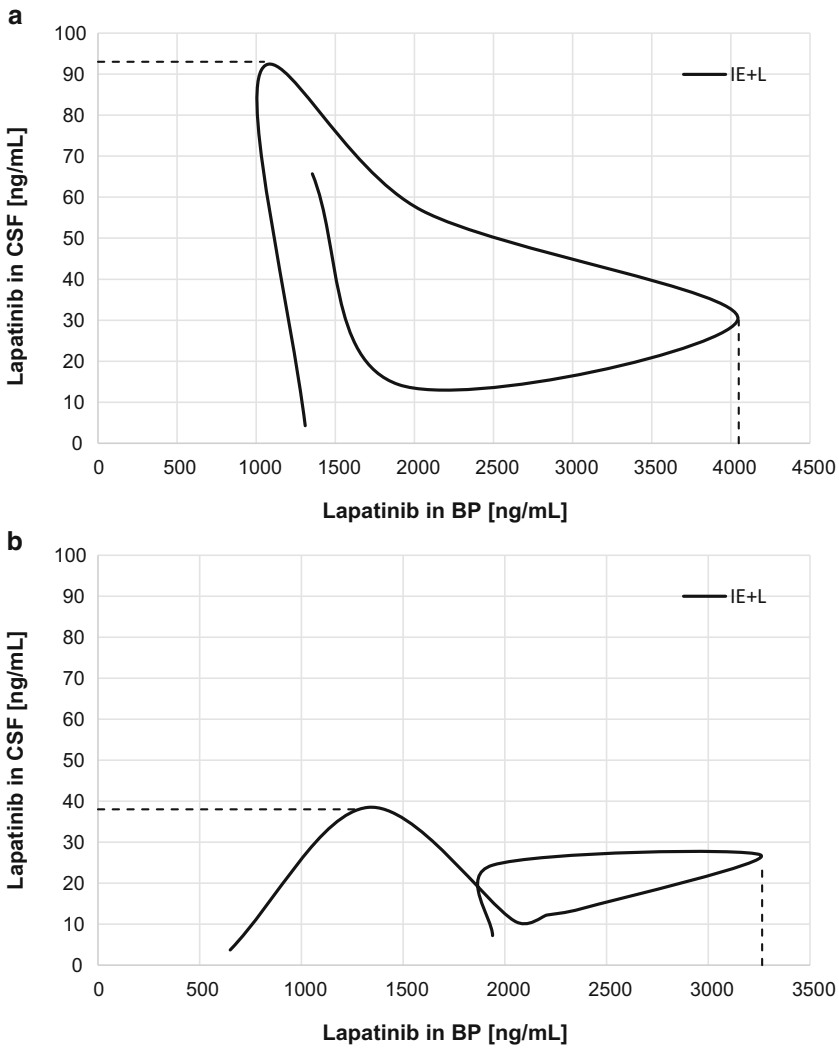

Fig. 5 The comparative hysteresis-like plots of the lapatinib concentration in the cerebrospinal fluid (CSF) versus blood plasma (BP) for the I_{E+L} group, $r^2 = 0.1665$ (**a**) and for the II_L group, $r^2 = 0.0183$ (**b**)

of this TKI in the *abcbla/lb*$^{(-/-)}$ mice was approximately 70 times greater than in the WT mice. It is noteworthy that the oral administration of elacridar enhanced the plasma and brain concentrations of crizotinib as well as the brain to plasma concentration ratio in WT mice, which is comparable to that of the *abcbla/1b;abcg2*$^{(-/-)}$ mice. The authors concluded that the administration of elacridar with crizotinib could significantly increase the bioavailability and penetration of crizotinib to the BT, and this combination therapy may be used in clinical practice to potentiate crizotinib efficacy in patients with non-small-cell lung cancer and BM.

Oberoi et al. [19] observed that the DTI_{BT} of sunitinib was 3.9 in *mdr1a/b*$^{(-/-)}$ mice and 2.1 in *bcrp1*$^{(-/-)}$ mice, whereas in mice with both knockout genes, the DTI_{BT} value increased to 48.9. Similarly, Polli et al. [31] showed that after 24-h intravenous administration of lapatinib, the $K_{p,BT}$ value was only 0.04 in WT mice, but it was 40 times greater in *mdr1a/b*$^{(-/-)}$*/bcrp*$^{(-/-)}$ mice. These results suggested that both P-gp and BCRP synergistically contributed to the penetration of lapatinib in the brain. Blocking P-gp and BCRP activity with elacridar may be a promising option for increasing the efficacy of TKIs, including lapatinib, in the treatment of brain tumors.

Our study was significantly limited by the fact that the unbound drug fraction in the BP, CSF and BT was not measured. Nonetheless, 99% of lapatinib binds with plasma proteins, mainly with albumin and alpha-1 acid glycoprotein. Thus, the unbound fraction is only 1% [32]. We did not use animals with the knockout genotype (*mdr1a/b*$^{(-/-)}$*,bcrp1*$^{(-/-)}$) to bring the study conditions closer to the physiological state.

Conclusion

The study proved that elacridar influences the pharmacokinetics of lapatinib. The inhibition of ABCB1 and ABCG2 transporters by elacridar substantially enhanced the penetration of lapatinib into the CSF and BT. Blocking protein transporters is a promising method of increasing the CNS disposition of TKIs and could become an indispensable part of the treatment

of patients with BC and brain (micro) metastases behind a functionally intact BBB.

Funding The study was financed with an academic grant of the Poznań University of Medical Sciences (grant No. 502–01–33114230-03592). The funding source had no effect on any part of the study, preparation or submission of the manuscript.

Compliance with ethical standards

Conflict of interest Author AK declares no conflict of interest. Author KS declares no conflict of interest. Author WP declares no conflict of interest. Author TG declares no conflict of interest. Author AK declares no conflict of interest. Author SP declares no conflict of interest. Author EG declares no conflict of interest. Author ES declares no conflict of interest.

Ethical approval All applicable international, national, and/or institutional guidelines concerning the care and use of animals were followed.

Informed consent No formal consent is required for this type of study.

References

1. Redig AJ, McAllister SS (2013) Breast cancer as a systemic disease: a view of metastasis. J Intern Med 274(2):113–126. https://doi.org/10.1111/joim.12084
2. Schouten LJ, Rutten J, Huveneers HA, Twijnstra A (2002) Incidence of brain metastases in a cohort of patients with carcinoma of the breast, colon, kidney, and lung and melanoma. Cancer 94(10):2698–2705
3. Stemmler HJ, Heinemann V (2008) Central nervous system metastases in HER-2-overexpressing metastatic breast cancer: a treatment challenge. Oncologist 13(7):739–750. https://doi.org/10.1634/theoncologist.2008-0052
4. Kühnöl J, Kühnöl C, Vordermark D (20016) Radiotherapy of brain metastases from breast cancer: treatment results and prognostic factors. Oncol Lett 11(5):3223–3227
5. Hurvitz SA, O'Shaughnessy J, Mason G, Yardley D, Jahanzeb M, Brufsky AM, Rugo HS, Swain SM, Kaufman PA, Tripathy D, Chu L, Li H, Antao V, Cobleigh M (2018) Central nervous system metastasis in patients with HER2-positive metastatic breast Cancer: patient characteristics, treatment, and survival from SystHERs. Clin Cancer Res pii: clincanres.2366.2018. https://doi.org/10.1158/1078-0432.CCR-18-2366
6. Petrelli F, Ghidini M, Lonati V, Tomasello G, Borgonovo K, Ghilardi M, Cabiddu M, Barni S (2017) The efficacy of lapatinib and capecitabine in HER-2 positive breast cancer with brain metastases: a systematic review and pooled analysis. Eur J Cancer 84:141–148. https://doi.org/10.1016/j.ejca.2017.07.024
7. Canonici A, Qadir Z, Conlon NT, Collins DM, O'Brien NA, Walsh N, Eustace AJ, O'Donovan N, Crown J (2018) The HSP90 inhibitor NVP-AUY922 inhibits growth of HER2 positive and trastuzumab-resistant breast cancer cells. Investig New Drugs 36(4):581–589. https://doi.org/10.1007/s10637-017-0556-7
8. Medina PJ, Goodin S (2008) Lapatinib: a dual inhibitor of human epidermal growth factor receptor tyrosine kinases. Clin Ther 30(8):1426–1447. https://doi.org/10.1016/j.clinthera.2008.08.008
9. Koo T, Kim IA (2016) Brain metastasis in human epidermal growth factor receptor 2-positive breast cancer: from biology to treatment. Radiat Oncol J 34(1):1–9. https://doi.org/10.3857/roj.2016.34.1.1
10. Liao J, Gallas M, Pegram M, Slingerland J (2010) Lapatinib: new opportunities for management of breast cancer. Breast Cancer (Dove Med Press) 15(2):79–91. https://doi.org/10.2147/BCTT.S5929
11. Gril B, Palmieri D, Bronder JL, Herring JM, Vega-Valle E, Feigenbaum L, Liewehr DJ, Steinberg SM, Merino MJ, Rubin SD, Steeg PS (2008) Effect of lapatinib on the outgrowth of metastatic breast cancer cells to the brain. J Natl Cancer Inst 100(15):1092–1103. https://doi.org/10.1093/jnci/djn216
12. Taskar KS, Rudraraju V, Mittapalli RK, Samala R, Thorsheim HR, Lockman J, Gril B, Hua E, Palmieri D, Polli JW, Castellino S, Rubin SD, Lockman PR, Steeg PS, Smith QR (2012) Lapatinib distribution in HER2 overexpressing experimental brain metastases of breast cancer. Pharm Res 29(3):770–781. https://doi.org/10.1007/s11095-011-0601-8
13. van der Noll R, Smit WM, Wymenga AN, Boss DS, Grob M, Huitema AD, Rosing H, Tibben MM, Keessen M, Rehorst H, Beijnen JH, Schellens JH (2015) Phase I and pharmacological trial of lapatinib in combination with gemcitabine in patients with advanced breast cancer. Investig New Drugs 33(6):1197–1205. https://doi.org/10.1007/s10637-015-0281-z
14. Zhang J, Zhang L, Yan Y, Li S, Xie L, Zhong W, Lv J, Zhang X, Bai Y, Cheng Z (2015) Are capecitabine and the active metabolite 5-Fu CNS penetrable to treat breast cancer brain metastasis? Drug Metab Dispos 43(3):411–417. https://doi.org/10.1124/dmd.114.061820
15. Montesinos RN, Moulari B, Gromand J, Beduneau A, Lamprecht A, Pellequer Y (2014) Coadministration of P-glycoprotein modulators on loperamide pharmacokinetics and brain distribution. Drug Metab Dispos 42(4):700–706. https://doi.org/10.1124/dmd.113.055566
16. Kallem R, Kulkarni CP, Patel D, Thakur M, Sinz M, Singh SP, Mahammad SS, Mandlekar S (2012) A simplified protocol employing elacridar in rodents: a screening model in drug discovery to assess P-gp mediated efflux at the blood brain barrier. Drug Metab Lett 6(2):134–144
17. Nakamura Y, Hirokawa Y, Kitamura S, Yamasaki W, Arihiro K, Tatsugami F, Iida M, Kakizawa H, Date S, Awai K (2013) Effect of lapatinib on hepatic parenchymal enhancement on gadoxetate disodium (EOB)-enhanced MRI scans of the rat liver. Jpn J Radiol 31(6):386–392. https://doi.org/10.1007/s11604-013-0208-6
18. Fridén M, Ljungqvist H, Middleton B, Bredberg U, Hammarlund-Udenaes M (2010) Improved measurement of drug exposure in the brain using drug-specific correction for residual blood. J Cereb Blood Flow Metab 30(1):150–161. https://doi.org/10.1038/jcbfm.2009.200
19. Oberoi RK, Mittapalli RK, Elmquist WF (2013) Pharmacokinetic assessment of efflux transport in sunitinib distribution to the brain. J Pharmacol Exp Ther 347(3):755–764. https://doi.org/10.1124/jpet.113.208959
20. Franchino F, Rudà R, Soffietti R (2018) Mechanisms and therapy for Cancer metastasis to the brain. Front Oncol 8:161. https://doi.org/10.3389/fonc.2018.00161
21. Verheijen RB, Yaqub M, Sawicki E, van Tellingen O, Lammertsma AA, Nuijen B, Schellens JHM, Beijnen JH, Huitema ADR, Hendrikse NH, Steeghs N (2018) Molecular imaging of ABCB1 and ABCG2 inhibition at the human blood-brain barrier using Elacridar and ^{11}C-Erlotinib PET. J Nucl Med 59(6):973–979. https://doi.org/10.2967/jnumed.117.195800

22. Goutal S, Gerstenmayer M, Auvity S, Caillé F, Mériaux S, Buvat I, Larrat B, Tournier N (2018) Physical blood-brain barrier disruption induced by focused ultrasound does not overcome the transporter-mediated efflux of erlotinib. J Control Release 292:210–220. https://doi.org/10.1016/j.jconrel.2018.11.009
23. Kort A, Durmus S, Sparidans RW, Wagenaar E, Beijnen JH, Schinkel AH (2015) Brain and testis accumulation of Regorafenib is restricted by breast Cancer resistance protein (BCRP/ABCG2) and P-glycoprotein (P-GP/ABCB1). Pharm Res 32(7):2205–2216. https://doi.org/10.1007/s11095-014-1609-7
24. Lagas JS, van Waterschoot RA, van Tilburg VA, Hillebrand MJ, Lankheet N, Rosing H, Beijnen JH, Schinkel AH (2009) Brain accumulation of dasatinib is restricted by P-glycoprotein (ABCB1) and breast cancer resistance protein (ABCG2) and can be enhanced by elacridar treatment. Clin Cancer Res 15(7):2344–2351. https://doi.org/10.1158/1078-0432.CCR-08-2253
25. Tang SC, Nguyen LN, Sparidans RW, Wagenaar E, Beijnen JH, Schinkel AH (2014) Increased oral availability and brain accumulation of the ALK inhibitor crizotinib by coadministration of the P-glycoprotein (ABCB1) and breast cancer resistance protein (ABCG2) inhibitor elacridar. Int J Cancer 134(6):1484–1494. https://doi.org/10.1002/ijc.28475
26. Gori S, Lunardi G, Inno A, Foglietta J, Cardinali B, Del Mastro L, Crinò L (2014) Lapatinib concentration in cerebrospinal fluid in two patients with HER2-positive metastatic breast cancer and brain metastases. Ann Oncol 25(4):912–913. https://doi.org/10.1093/annonc/mdu041
27. Devriese LA, Koch KM, Mergui-Roelvink M, Matthys GM, Ma WW, Robidoux A, Stephenson JJ, Chu QS, Orford KW, Cartee L, Botbyl J, Arya N, Schellens JH (2014) Effects of low-fat and high-fat meals on steady-state pharmacokinetics of lapatinib in patients with advanced solid tumours. Investig New Drugs 32(3):481–488. https://doi.org/10.1007/s10637-013-0055-4
28. Polli JW, Humphreys JE, Harmon KA, Castellino S, O'Mara MJ, Olson KL, John-Williams LS, Koch KM, Serabjit-Singh CJ (2008) The role of efflux and uptake transporters in *N*-{3-Chloro-4-[(3-fluorobenzyl)oxy]phenyl}-6-[5-({[2-(methylsulfonyl)ethyl]amino}methyl)-2-furyl]-4-quinazolinamine (GW572016, Lapatinib) disposition and drug interactions. Drug Metab Dispos 36(4):695–701. https://doi.org/10.1124/dmd.107.018374
29. Sato H, Siddig S, Uzu M, Suzuki S, Nomura Y, Kashiba T, Gushimiyagi K, Sekine Y, Uehara T, Arano Y, Yamaura K, Ueno K (2015) Elacridar enhances the cytotoxic effects of sunitinib and prevents multidrug resistance in renal carcinoma cells. Eur J Pharmacol 746:258–266. https://doi.org/10.1016/j.ejphar.2014.11.021
30. Ward KW, Azzarano LM (2004) Preclinical pharmacokinetic properties of the P-glycoprotein inhibitor GF120918A (HCl salt of GF120918, 9,10-dihydro-5-methoxy-9-oxo-N-[4-[2-(1,2,3,4-tetrahydro-6,7-dimethoxy-2-isoquinolinyl)ethyl]phenyl]-4-acridine-carboxamide) in the mouse, rat, dog, and monkey. J Pharmacol Exp Ther 310(2):703–709. https://doi.org/10.1124/jpet.104.068288
31. Polli JW, Olson KL, Chism JP, John-Williams LS, Yeager RL, Woodard SM, Otto V, Castellino S, Demby VE (2009) An unexpected synergist role of P-glycoprotein and breast cancer resistance protein on the central nervous system penetration of the tyrosine kinase inhibitor lapatinib (N-{3-chloro-4-[(3-fluorobenzyl)oxy]phenyl}-6-[5-({[2-(methylsulfonyl)ethyl]amino}methyl)-2-furyl]-4-quinazolinamine; GW572016). Drug Metab Dispos 37(2):439–442. https://doi.org/10.1124/dmd.108.024646
32. Hudachek SF, Gustafson DL (2013) Physiologically based pharmacokinetic model of lapatinib developed in mice and scaled to humans. J Pharmacokinet Pharmacodyn 40(2):157–176. https://doi.org/10.1007/s10928-012-9295-8